

NASA TECHNICAL NOTE



NASA TN D-3285

NASA TN D-3285

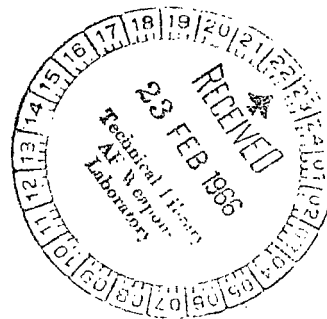
e.1
LOAN COPY:
AFWL
KIRTLAND AFB



TECH LIBRARY KAFB, NM
TO
X

**FLOW FIELD SURVEY AND
DECCELERATOR DRAG CHARACTERISTICS
IN THE WAKE OF A MODEL OF THE
X-15 AIRPLANE AT MACH 2.30 AND 4.65**

*by James F. Campbell
Langley Research Center
Langley Station, Hampton, Va.*





FLOW FIELD SURVEY AND DECELERATOR DRAG CHARACTERISTICS
IN THE WAKE OF A MODEL OF THE X-15 AIRPLANE

AT MACH 2.30 AND 4.65

By James F. Campbell

Langley Research Center
Langley Station, Hampton, Va.

NATIONAL AERONAUTICS AND SPACE ADMINISTRATION

For sale by the Clearinghouse for Federal Scientific and Technical Information
Springfield, Virginia 22151 - Price \$2.00

FLOW FIELD SURVEY AND DECELERATOR DRAG CHARACTERISTICS

IN THE WAKE OF A MODEL OF THE X-15 AIRPLANE

AT MACH 2.30 AND 4.65

By James F. Campbell
Langley Research Center

SUMMARY

An investigation was made to determine decelerator drag characteristics in the asymmetric wake of a 1/12-scale model of the X-15 airplane at a Mach number of 4.65. The four types of decelerators tested were as follows: Self-inflatable (ram-air) ballute, supersonic parachute, rigid cone, and rigid tension shell. A pressure survey was also included at Mach numbers of 2.30 and 4.65 to define the X-15 wake characteristics.

Decelerators are available that will produce stable characteristics behind the X-15 airplane and with relatively high drag characteristics, even though the X-15 has asymmetric wake characteristics. At trailing distances on the order of 7 to 10 times the towing-model base diameter, the 80° rigid cone had the highest value of drag coefficient of all the decelerator configurations investigated. Both the rigid tension-shell configuration and the supersonic parachute configuration were extremely unstable at longitudinal distances downstream of the towing-vehicle base greater than 4.5 and 6.7 base diameters, respectively; however, the tension-shell configuration indicated a potentially high drag capability.

INTRODUCTION

The use of towed decelerators for controlled reentry and/or recovery of spacecraft and other high-speed vehicles establishes the criterion of satisfactory performance at high altitudes and supersonic speeds. Wind-tunnel studies at supersonic and hypersonic speeds have been made on a variety of decelerator configurations (refs. 1 to 8) and have indicated satisfactory drag and stability characteristics for several types of decelerators. These investigations were undertaken with the decelerators attached to missile or spacecraft configurations as the towing vehicle, and it is felt desirable to determine whether these same types of decelerators are feasible for use on an airplane configuration. Since airplane wakes have some degree of asymmetry as compared with missile wakes and since the X-15 airplane fits in the broad category of hypersonic entry vehicles, a model

of this airplane was believed appropriate for these tests. An experimental study, therefore, was made of several types of decelerators attached to a 1/12-scale model of the X-15 airplane as the towing vehicle. In order to understand decelerator performance more completely, a pressure survey was also included to define the wake characteristics behind the model. An off-center tow position for the decelerators was dictated by the engine arrangement on the airplane.

The four types of decelerators tested were as follows: Self-inflatable (ram-air) ballute, supersonic parachute, rigid cone, and rigid tension shell. The tests were performed in the Langley Unitary Plan wind tunnel at a Mach number of 4.65 for the decelerator-drag study and at Mach numbers of 2.30 and 4.65 for the X-15 wake survey.

SYMBOLS

Measurements for this investigation were taken in the U.S. Customary System of Units. Equivalent values are indicated herein parenthetically in the International System (SI) in the interest of promoting use of this system in future NASA reports. Details concerning the use of SI, together with physical constants and conversion factors, are given in reference 9.

- A reference area (maximum cross-sectional area of decelerator, based on maximum diameter a ; includes burble fence on B₁, B₂, and B₃ configurations)
- a maximum diameter of decelerator
- b diameter of maximum cross section of self-inflatable decelerator excluding burble fence
- c distance from apex of self-inflatable decelerator to point of maximum cross section (excluding burble fence), measured parallel to center line
- C_D drag coefficient, D/qA
- D drag
- d base diameter of towing vehicle
- e length of self-inflatable decelerator
- f width of inflation scoop on self-inflatable decelerator

g	height in radial direction of inflation scoop on B ₂ and B ₃ self-inflatable decelerator configurations
l	local length
M	free-stream Mach number
p	static pressure
p _t	total pressure (behind a normal shock)
q	free-stream dynamic pressure
R/ft	Reynolds number per foot
R/m	Reynolds number per meter
r	local radius
x	longitudinal distance downstream of towing-vehicle base (for wake survey, measured to static- and total-pressure orifices; for decelerator-drag study, measured to apex of decelerator)
y	lateral distance from plane of symmetry of towing vehicle
z	vertical distance from center line of towing vehicle

APPARATUS

Wind Tunnel

The tests were conducted in the high Mach number test section of the Langley Unitary Plan wind tunnel, which is a variable-pressure continuous-flow tunnel. The test section is 4 feet (1.2 meters) square and 7 feet (2.1 meters) long. The nozzle leading to the test section is of the asymmetric, sliding-block type which permits a continuous variation in test-section Mach number from about 2.3 to 4.7.

Models

Airplane model.- Details of the 1/12-scale model (1/12th except for nose geometry) of the X-15 airplane are shown in figure 1. Emphasis was given to afterbody details

since this is the region of the towing vehicle most likely to affect the wake characteristics, which would, in turn, affect the drag and stability of a towed decelerator. The model was supported in the center of the tunnel by two thin struts spanning the tunnel in the horizontal plane. In order to simulate decelerator storage, a container was mounted on top of the fuselage rearward of the vertical fin.

Arrangement of the wire-strain-gage balance and the low-speed gear-reduction motor in the rear section of the model is shown in figure 2. The motor-driven drum was remotely operated and provided variation in the steel, tow-cable length. One suitable location for attachment of a tow cable on the X-15 flight vehicle is the upper engine mount. This location results in an off-center tow position which was simulated on the model by use of a pulley (fig. 2).

Decelerator models.- The following table lists the designation associated with each decelerator along with its maximum diameter and reference area:

Decelerator	Maximum diameter, a		Reference area, A	
	in.	cm	ft ²	m ²
B ₁	3.600	9.144	0.070686	0.006567
B ₂	5.875	14.923	.188253	.017489
B ₃	11.875	30.163	.769123	.071454
80° rigid cone	4.00	10.16	.087267	.008107
Supersonic parachute	3.50	8.89	.066814	.006207
Tension shell	4.00	10.16	.087267	.008107

Details of the self-inflatable (ram-air) ballute decelerator configurations (B₁, B₂, and B₃) are shown in figure 3. These models were fabricated from either nylon or dacron cloth and were coated with neoprene, which acted as a seal and eliminated porosity as a variable. There are four inflation scoops evenly spaced around the decelerators at the point of maximum cross section (excluding the burble fence). The nylon cords shown in figure 3 were glued to the decelerator surface.

Three other decelerator test models are shown in figure 4. The rigid cone and tension-shell models were made of fiber glass; the supersonic parachute model was constructed of wire mesh and close-woven cloth, with nylon shroud lines. (Details of a similar supersonic parachute configuration are shown in ref. 8.) Ordinates defining the shape of the tension-shell configuration are presented in table I.

A swivel was used in attaching the decelerator models to the tow cable to allow decelerator rolling motion without inducing twisting loads in the cable. A line attached to the rear of all the decelerators stabilized them during starting and stopping of the

tunnel and also prevented the models from striking the test-section windows during periods of instability. This line was kept slack during data acquisition. No attempt was made in this investigation to simulate decelerator mass or tow-cable mass and elastic properties; of course, simulating mutual dynamic characteristics between the forebody (X-15 model) and the decelerator was impossible under these test conditions.

TESTS

Test conditions for the flow survey behind the X-15 model are summarized in the following table:

Mach number	Stagnation temperature		Stagnation pressure		Dynamic pressure		Reynolds number	
	°F	°K	psf	kN/m ²	psf	kN/m ²	per ft	per m
2.30	150	339	1189	56.930	352	16.854	1.56×10^6	5.12×10^6
4.65	175	353	7716	369.444	336	16.088	2.91	9.55

Drag data were obtained on the decelerator models at $M = 4.65$; the test conditions are as follows:

Stagnation temperature		Stagnation pressure		Dynamic pressure		Reynolds number	
°F	°K	psf	kN/m ²	psf	kN/m ²	per ft	per m
175	353	4262	204.066	185	8.858	1.61×10^6	5.28×10^6
175	353	7727	369.971	335	16.040	2.91	9.55
175	353	12274	587.682	533	25.520	4.63	15.19

Drag data at a Reynolds number per foot of 2.91×10^6 ($R/m = 9.55 \times 10^6$) were obtained on the 80° cone, the B₁, and the B₃ configurations at $x/d = 7.70$; in addition, the B₁ configuration was tested at a Reynolds number per foot of 4.63×10^6 ($R/m = 15.19 \times 10^6$) at $x/d = 10.08$.

The stagnation dewpoint was maintained below -30° F (239° K) in order to avoid condensation effects in the test section.

MEASUREMENTS AND ACCURACY

Decelerator drag force was measured by means of an electrical strain-gage balance housed within the X-15 model and rigidly fastened to the drum and pulley support.

A pressure rake was used to perform the wake survey behind the X-15 model and is illustrated in figure 5. The rake was 10 inches (25.4 cm) high and was composed of 41 total-pressure probes 1/4 inch (0.635 cm) apart and 21 static-pressure probes 1/2 inch (1.270 cm) apart. Pressure measurements were obtained by means of pressure transducers. In addition to force data, high-speed schlieren motion pictures were taken of each decelerator model. Schlieren photographs of the pressure rake and the decelerator models at various x/d locations behind the X-15 model are shown in figures 6 and 7, respectively.

The accuracies of the individual quantities are estimated to be within the following limits:

C_D	± 0.05
p	± 7 psf (± 335 N/m ²)
p_t	± 10 psf (± 479 N/m ²)
x , decelerator study	± 0.20 in. (± 0.508 cm)
x , wake survey	± 0.01 in. (± 0.025 cm)
y	± 0.01 in. (± 0.025 cm)
z	± 0.01 in. (± 0.025 cm)

DISCUSSION

Wake Survey

Total-pressure distributions in the vertical plane of symmetry at $M = 2.30$ and $M = 4.65$ are shown in figure 8 at various x/d locations behind the X-15 model base. The data indicate that at small values of x/d (0.25 and 0.42) and within the geometric limits of the model base ($z = \pm 2$ inches (± 5.08 cm)) the total pressures are essentially equal to base static pressure at both Mach numbers. This no-flow condition near the model base was referred to as the "dead-air region" in reference 10. As the value of x/d is increased, a corresponding increase is seen in total pressure near the model center line. At the largest value of x/d , the pressure recovery is about 75 percent of free-stream total pressure for $M = 2.30$ and about 60 percent of free-stream total pressure for $M = 4.65$. The large increase in p_t seen as z is increased negatively would be expected to occur at larger, positive z values because of X-15 geometry differences above and below the model center line. These data indicate the center of the wake to be located near a positive value of z between 1 inch (2.54 cm) and 2 inches (5.08 cm).

The vertical total- and static-pressure distributions at various distances from the model plane of symmetry ($y/d = 0$ to 2.75) are shown in figure 9 for each x/d location. As lateral distance is increased from $y/d = 0$ the asymmetric effects of the X-15 model

on total pressure rapidly dissipate, particularly outside the region near the model base (y/d equal to or greater than 0.5). At $y/d = 2.75$, only a small region near $z = 0$ shows a variation in p_t , probably as a result of the model support strut; the data presented in reference 10 for a cone-cylinder model using identical support struts indicated similar pressure distributions.

The total-pressure data indicate that the location of a decelerator in the wake of the X-15 model can be critical from the standpoint of decelerator drag and/or stability. The data (fig. 8) indicate that location of a decelerator at large distances from the X-15 base (at least 7.22 times the base diameter) is desirable for high drag characteristics. Since it would be expected that the wake will have the least effect on the stability characteristics of a decelerator located in the wake center, the off-center tow-cable attachment required for the X-15 configuration should be advantageous.

Drag and Stability

Tests in the Reynolds number range from 1.61×10^6 to 4.63×10^6 per foot (5.28×10^6 to 15.19×10^6 per m) at $M = 4.65$ indicated little effect of Reynolds number on the characteristics of the 80° rigid cone, the B₁, and the B₃ configurations. Variations of decelerator drag coefficient with trailing distance behind the X-15 model base are presented in figure 10 for each decelerator configuration tested at $M = 4.65$ for $R/\text{ft} = 1.61 \times 10^6$ ($R/\text{m} = 5.28 \times 10^6$) only. An increase in the value of x/d results in a general increase in C_D for all the decelerator configurations investigated. Data obtained as the trailing distance is decreased (ticked symbols) generally indicate higher values of C_D than did the data obtained at the corresponding location but with increasing trailing distances. This trend was also noted in reference 7 for several spherical models and was attributed to the decelerator's passing through the transition region of the wake. The differences shown in the present investigation, however, are considerably smaller than those shown in reference 7, probably because of the small diameter of the decelerator in comparison with the model base.

Effect of decelerator size on C_D can be seen by comparing the results for the B₁, B₂, and B₃ configurations, where increasing the maximum diameter from 3.600 inches (9.144 cm) for B₁ to 11.875 inches (30.163 cm) for B₃ results in corresponding increases in C_D throughout the x/d range. This trend (illustrated graphically in fig. 11) would be expected since increased diameter exposes larger portions of the decelerator area to the higher pressures that occur away from the center of the wake. It is believed that the difference in burble-fence and inflation-scoop geometries for the B₁ configuration as compared with those for the B₂ and B₃ configurations will not alter the drag and stability results presented herein.

At trailing distances on the order of 7 to 10 times the towing-model base diameter, the 80° rigid cone has the highest C_D value of all the decelerator configurations. Comparison of these 80° cone data with the data presented in references 5 and 7 for similar 80° cone configurations towed behind cone-cylinder models (center-line tow-cable attachment) shows that the cone of the present investigation has lower C_D values. It should be pointed out, however, that if comparable trailing-distance-to-base-diameter and decelerator-diameter-to-base-diameter ratios are considered (based on an X-15 model effective base diameter larger than 4 inches (10.16 cm), as indicated by the pressure results), comparable drag values might be attained. Comparison of the stability characteristics of these cone configurations by means of visual observation showed little difference in stability trends with x/d , particularly in the region of maximum C_D where the 80° cone configurations were stable regardless of the towing vehicle (X-15 model of the present investigation and cone-cylinder models of ref. 7). The ram-air decelerator configurations (B₁, B₂, and B₃) also showed a high degree of stability at large x/d values.

Although the tension-shell configuration indicates a potentially high drag capability, data were not obtained at x/d locations farther behind the forebody than are shown in figure 10 (that is, at x/d values greater than 4.5) because of severe oscillations of the model. Subsequent tests (unpublished data) have shown this tension-shell configuration to have similar instability characteristics when tethered behind a cone-cylinder model with a center-line tow cable. Similar oscillations were also noted for the supersonic parachute configuration, and resulted in termination of drag-data acquisition near x/d of 6.7.

CONCLUSIONS

A wind-tunnel investigation of the flow field and decelerator drag characteristics in the asymmetric wake of a 1/12-scale model of the X-15 airplane indicated the following conclusions:

1. Decelerators are available that will produce stable characteristics behind the X-15 airplane and with relatively high drag characteristics, even though the X-15 has asymmetric wake characteristics.
2. At trailing distances on the order of 7 to 10 times the towing-model base diameter, an 80° rigid cone had the highest value of drag coefficient of all the decelerator configurations investigated.

3. Both a rigid tension-shell configuration and a supersonic parachute configuration were extremely unstable at longitudinal distances downstream of the towing-vehicle base greater than 4.5 and 6.7 base diameters, respectively; however, the tension-shell configuration indicated a potentially high drag capability.

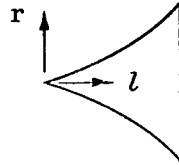
Langley Research Center,
National Aeronautics and Space Administration,
Langley Station, Hampton, Va., December 1, 1965.

REFERENCES

1. Nebiker, F. R.: Feasibility Study of an Inflatable Type Stabilization and Deceleration System for High Altitude and High-Speed Recovery. WADD Tech. Rept. 60-182, U.S. Air Force, Dec. 1961.
2. Aebischer, A. C.: Investigation To Determine the Feasibility of Using Inflatable Balloon Type Drag Devices for Recovery Applications in the Transonic, Supersonic, and Hypersonic Flight Regime - Part I. Functional and Performance Demonstration. ASD-TDR-62-702, Pt. 1, U.S. Air Force, Oct. 1962.
3. Alexander, W. C.: Investigation To Determine the Feasibility of Using Inflatable Balloon Type Drag Devices for Recovery Applications in the Transonic, Supersonic, and Hypersonic Flight Regime - Part II. Mach 4 to Mach 10 Feasibility Investigation. ASD-TDR-62-702, Pt. II, U.S. Air Force, Dec. 1962.
4. Coats, Jack D.: Static and Dynamic Testing of Conical Trailing Decelerators for the Pershing Re-Entry Vehicle. AEDC-TN-60-188, U.S. Air Force, Oct. 1960.
5. Charczenko, Nickolai; and McShera, John T.: Aerodynamic Characteristics of Towed Cones Used as Decelerators at Mach Numbers From 1.57 to 4.65. NASA TN D-994, 1961.
6. McShera, John T., Jr.: Aerodynamic Drag and Stability Characteristics of Towed Inflatable Decelerators at Supersonic Speeds. NASA TN D-1601, 1963.
7. Charczenko, Nickolai: Aerodynamic Characteristics of Towed Spheres, Conical Rings, and Cones Used as Decelerators at Mach Numbers From 1.57 to 4.65. NASA TN D-1789, 1963.
8. Charczenko, Nickolai: Wind-Tunnel Investigation of Drag and Stability of Parachutes at Supersonic Speeds. NASA TM X-991, 1964.
9. Mechtly, E. A.: The International System of Units - Physical Constants and Conversion Factors. NASA SP-7012, 1964.
10. McShera, John T., Jr.: Wind-Tunnel Pressure Measurements in the Wake of a Cone-Cylinder Model at Mach Numbers of 2.30 and 4.65. NASA TN D-2928, 1965.

TABLE I

ORDINATES DEFINING TENSION-SHELL MODEL



l		r	
		in.	cm
in.	cm	in.	cm
0.000	0.000	0.00	0.000
.210	.533	.10	.254
.422	1.072	.20	.508
.630	1.600	.30	.762
.832	2.113	.40	1.016
1.026	2.606	.50	1.270
1.218	3.094	.60	1.524
1.396	3.546	.70	1.778
1.562	3.967	.80	2.032
1.720	4.369	.90	2.286
1.864	4.735	1.00	2.540
1.996	5.070	1.10	2.794
2.116	5.375	1.20	3.048
2.216	5.629	1.30	3.302
2.308	5.862	1.40	3.556
2.384	6.055	1.50	3.810
2.448	6.218	1.60	4.064
2.496	6.340	1.70	4.318
2.530	6.426	1.80	4.572
2.554	6.487	1.90	4.826
2.562	6.507	2.00	5.080

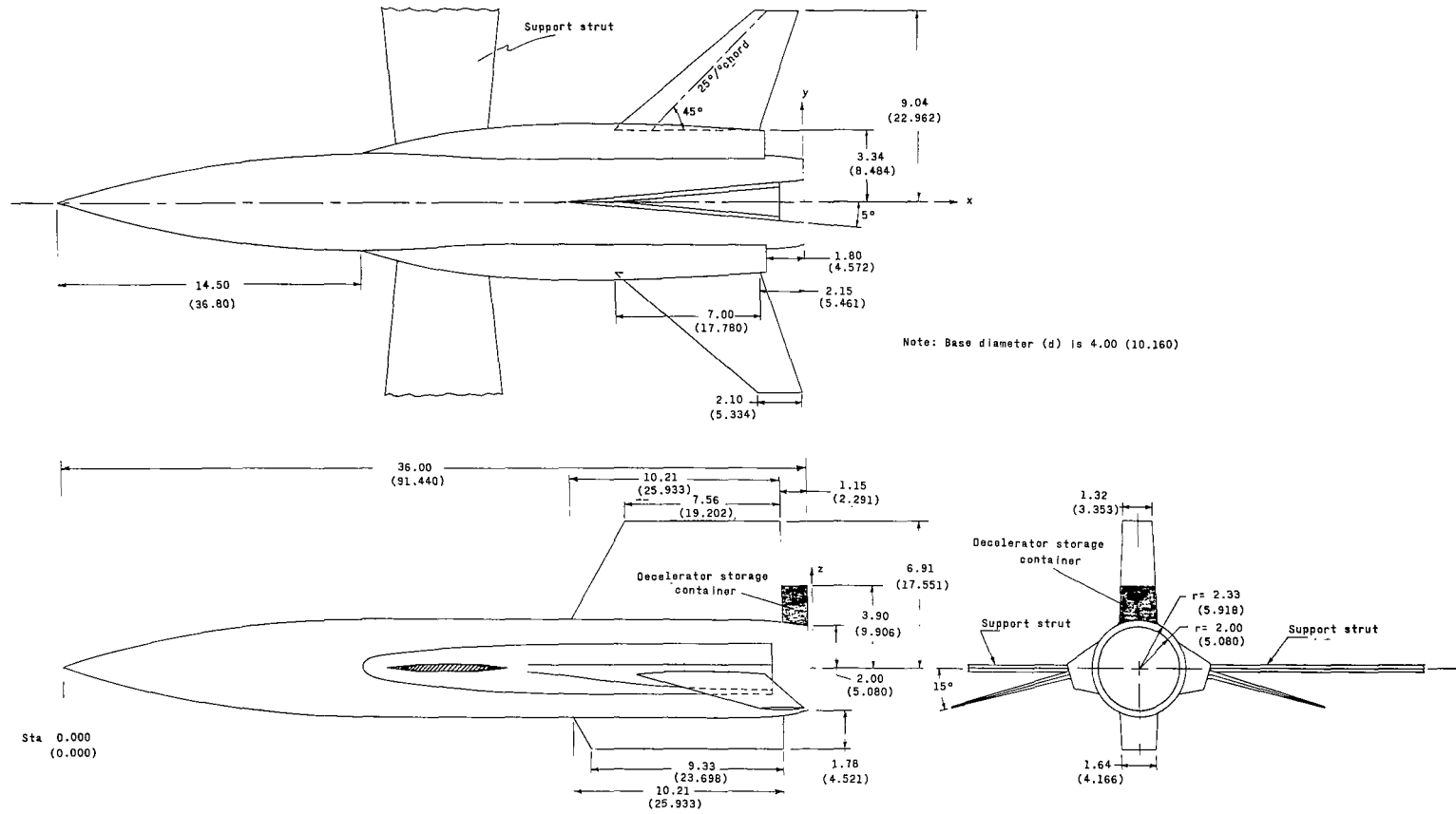


Figure 1.- X-15 details. (Dimensions are given first in inches and parenthetically in centimeters.)

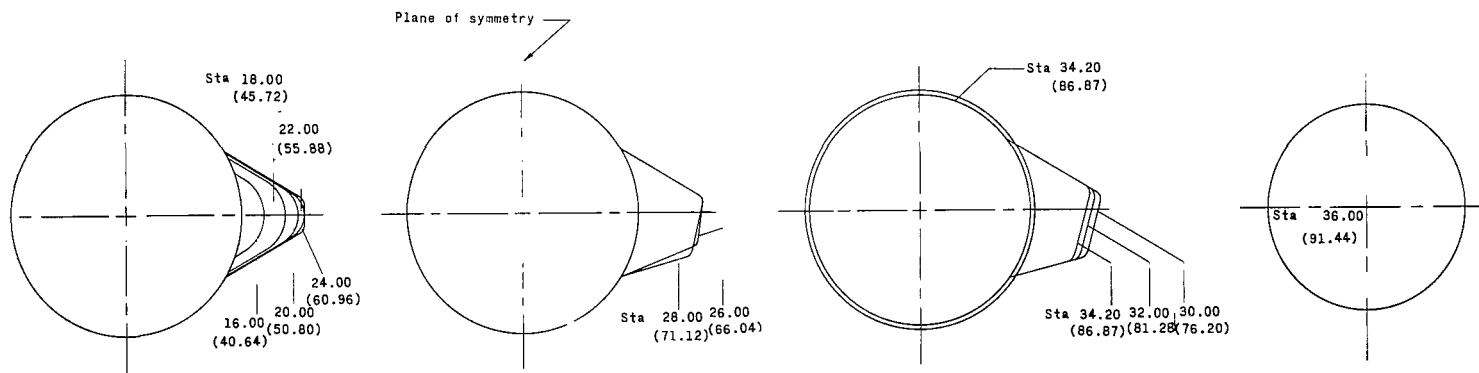
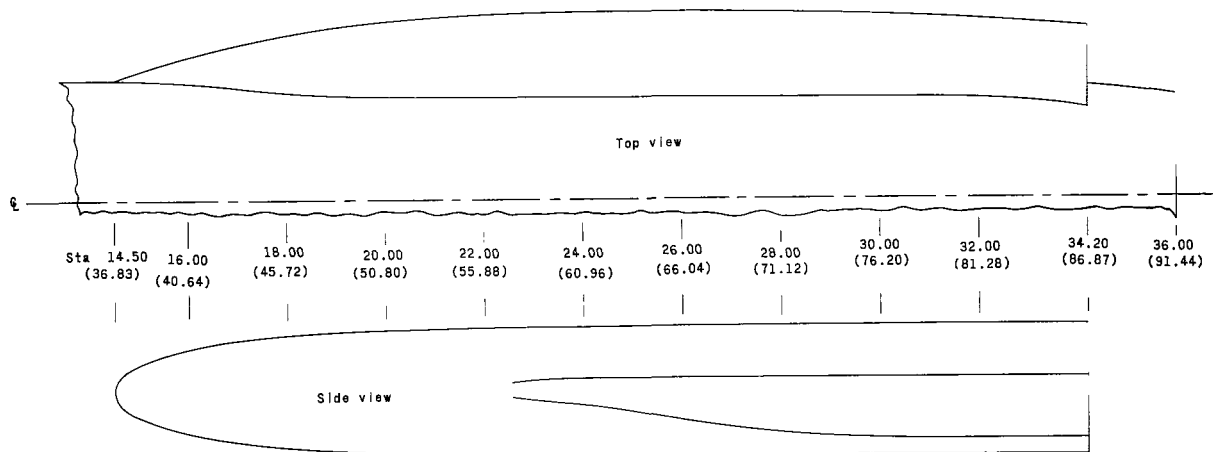


Figure 1.- Concluded.

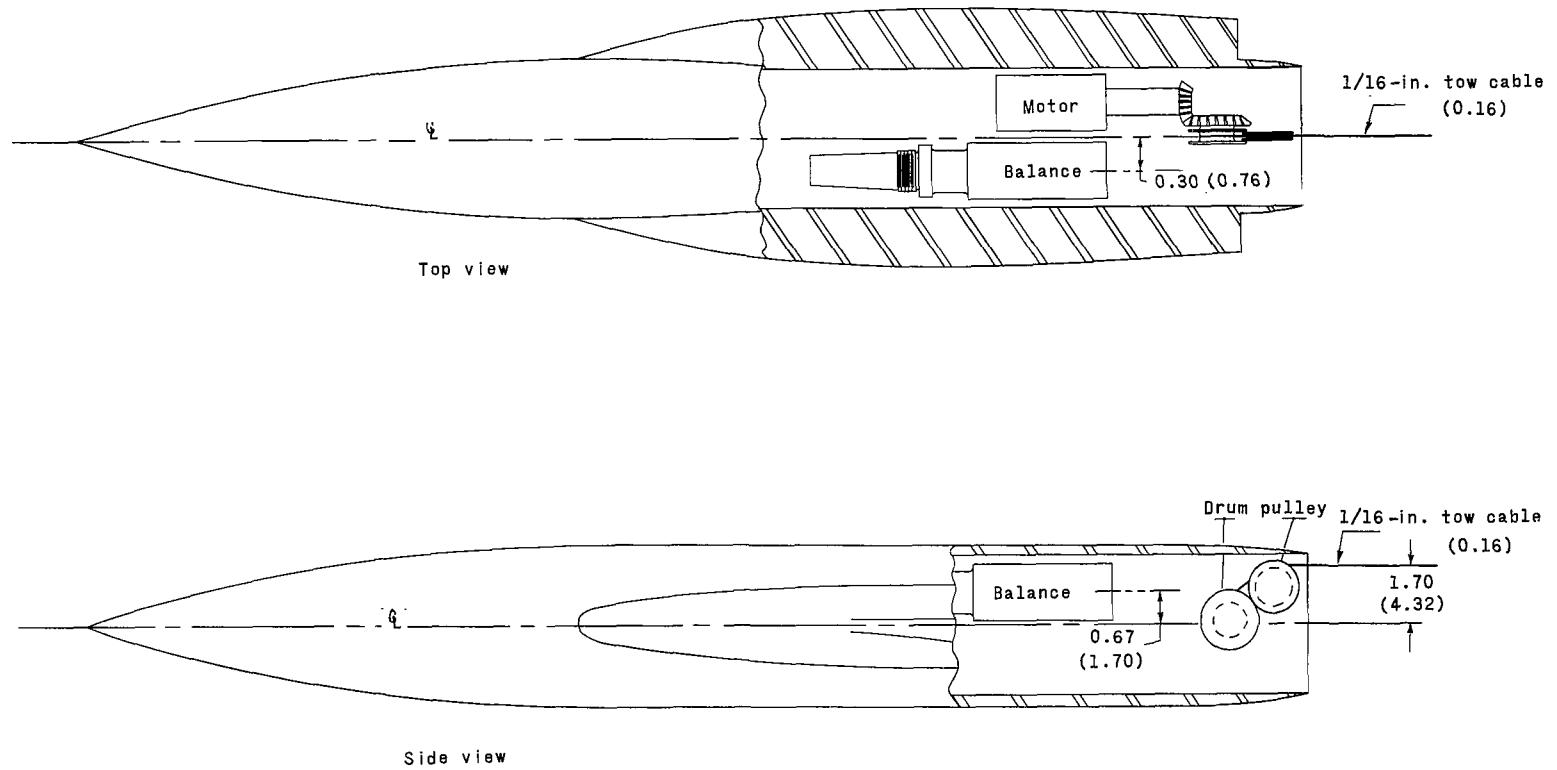
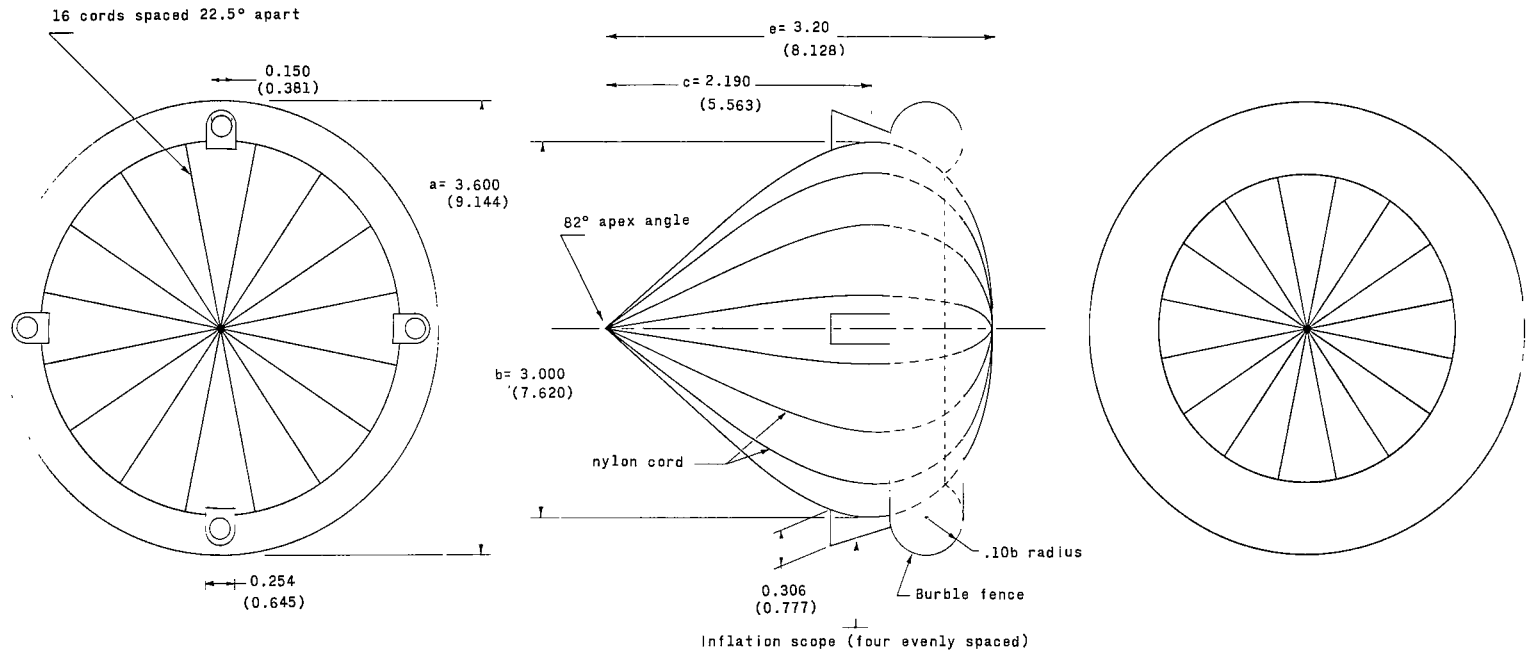
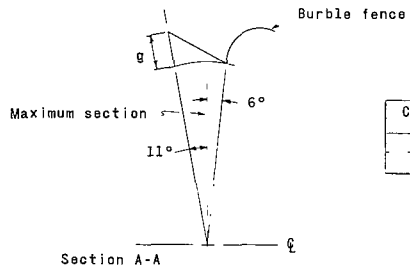
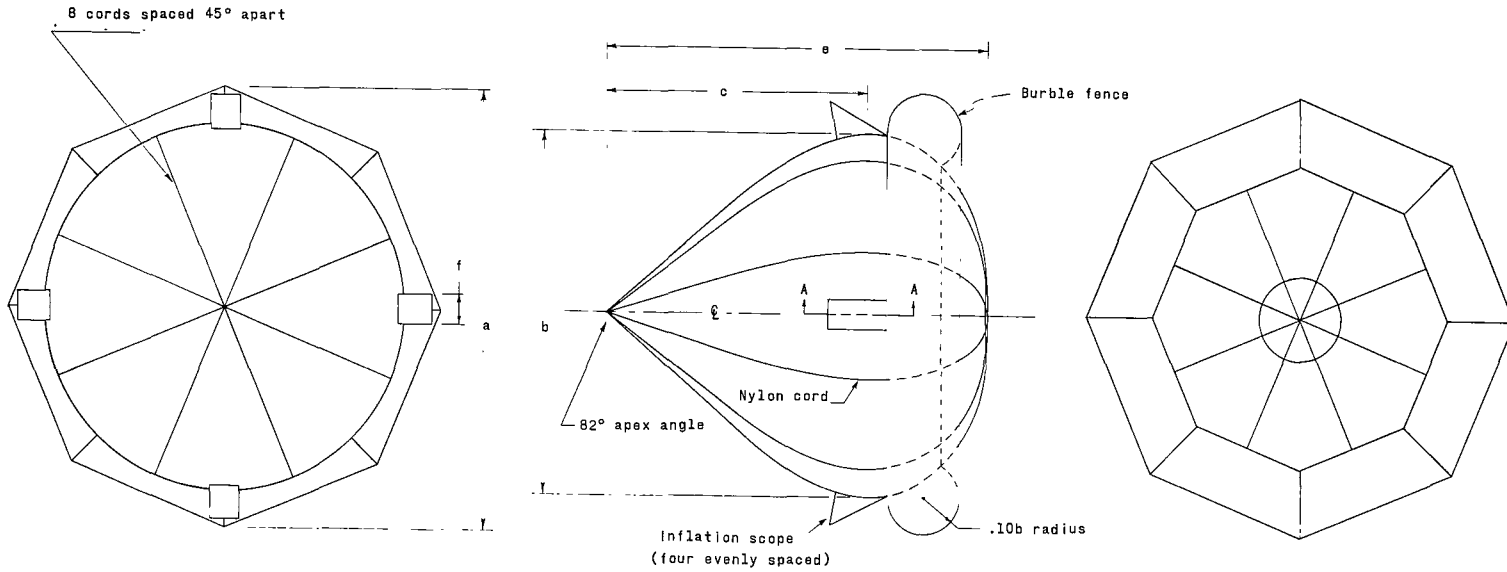


Figure 2.- X-15 internal arrangement. (Dimensions are given first in inches and parenthetically in centimeters.)



(a) B₁ configuration.

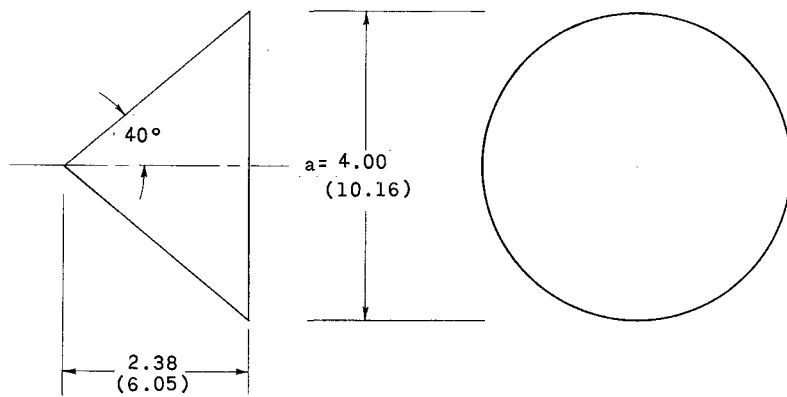
Figure 3.- Details of self-inflatable ballute decelerators. (Dimensions are given first in inches and parenthetically in centimeters.)



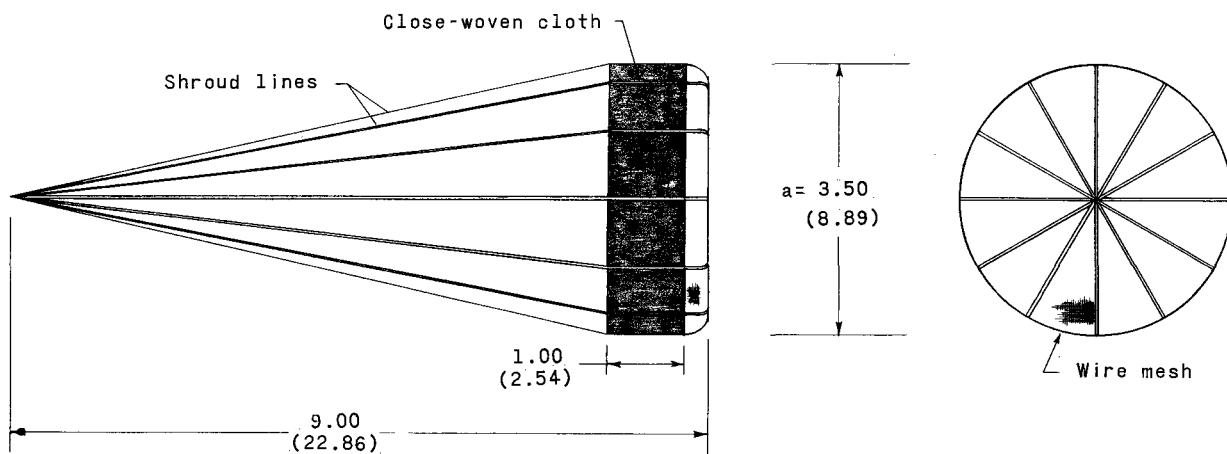
Configuration	a		b		c		e		f		g	
	in.	cm	in.	cm	in.	cm	in.	cm	in.	cm	in.	cm
B ₂	5.875	14.923	4.896	12.436	3.573	9.075	5.232	13.289	.396	1.006	.500	1.270
B ₃	11.875	30.163	9.896	25.136	7.222	18.344	10.576	26.863	.800	2.032	1.011	2.568

(b) B₂ and B₃ configurations.

Figure 3.- Concluded.

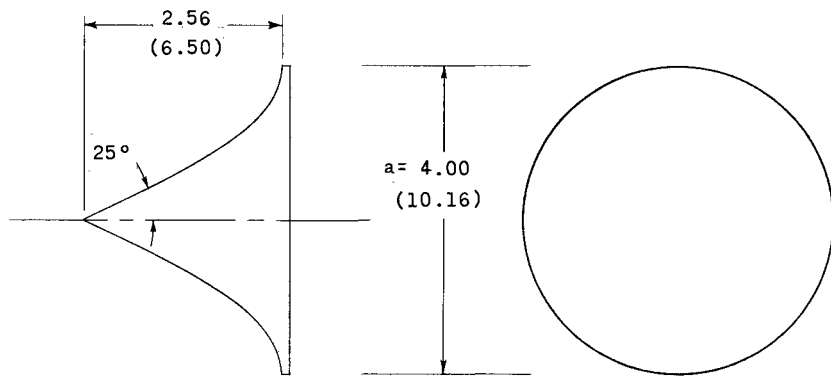


80° cone



Supersonic parachute

Note: Ordinates of tension-shell model are shown in table I



Tension shell

Figure 4.- Decelerator details. (Dimensions are given first in inches and parenthetically in centimeters.)

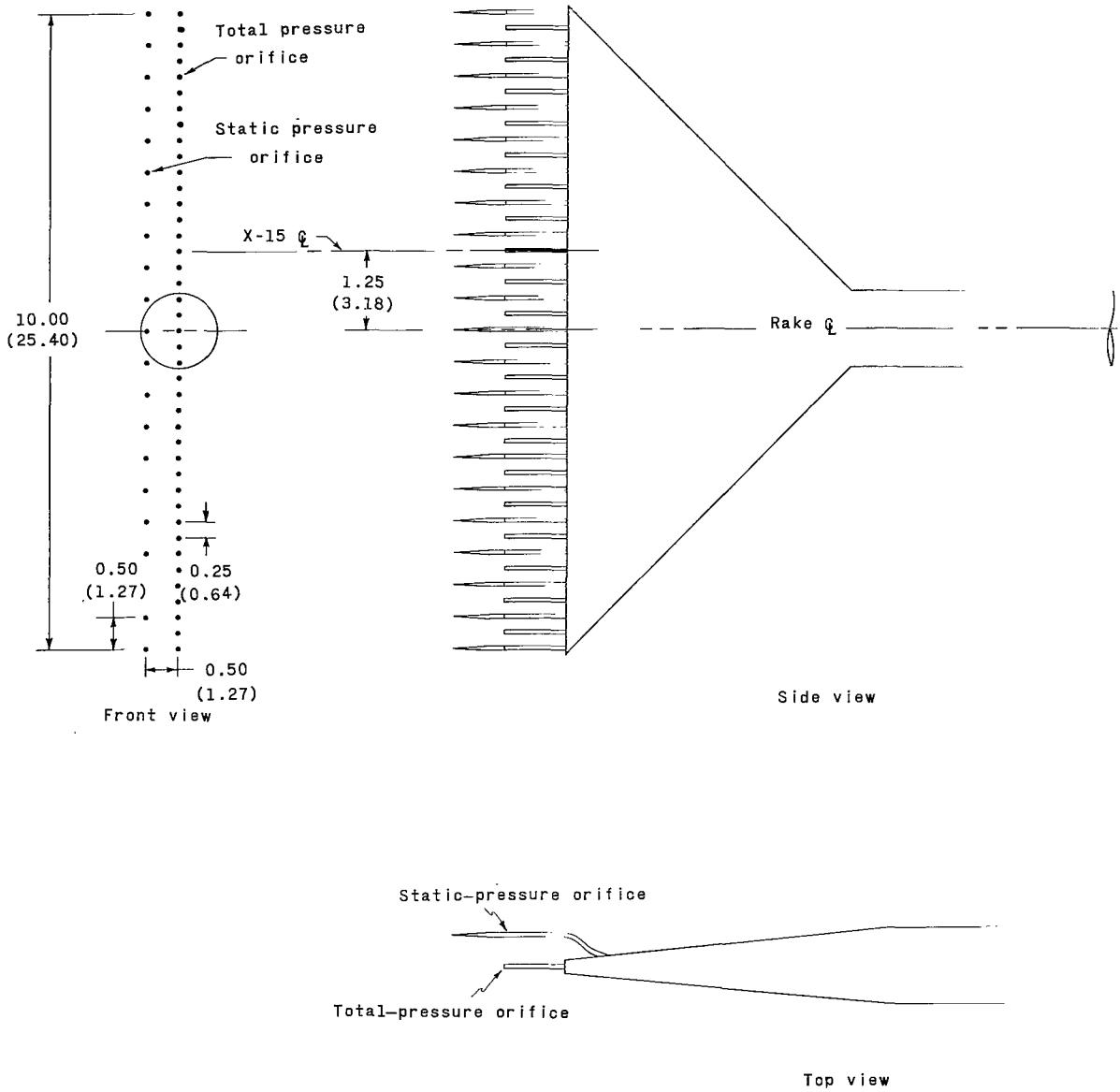
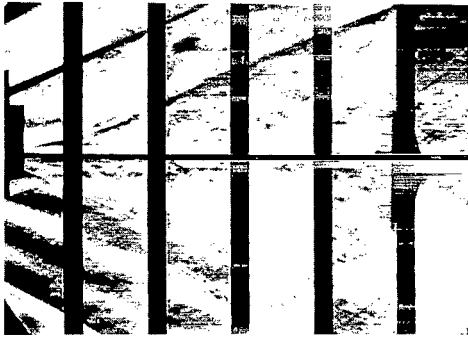
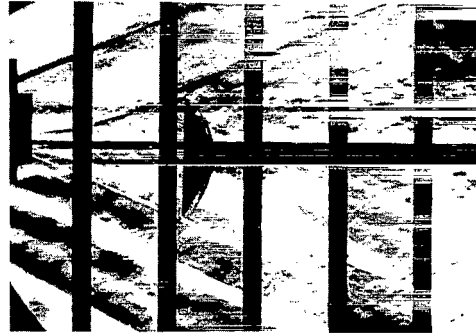


Figure 5.- Details of pressure rake. (Dimensions are given first in inches and parenthetically in centimeters.)



$x/d = 7.22$



$x/d = 2.52$



$x/d = 0.81$



$x/d = 0.42$



$x/d = 0.25$

(a) $M = 2.30$.

L-65-9031

Figure 6.- Schlieren photographs of pressure rake at various x/d locations behind the X-15 model.



$x/d = 7.22$



$x/d = 5.05$



$x/d = 2.52$



$x/d = 0.42$



$x/d = 0.25$

(b) $M = 4.65$.

L-65-9032

Figure 6.- Concluded.



$x/d \approx 7.63$



$x/d \approx 5.05$



$x/d = 2.55$

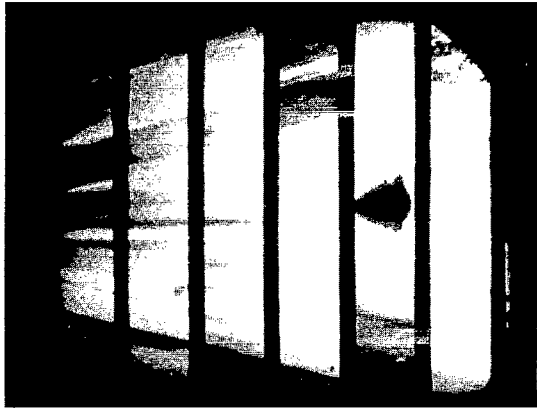


$x/d \approx 1.53$

(a) B₁ self-inflatable configuration.

L-65-9025

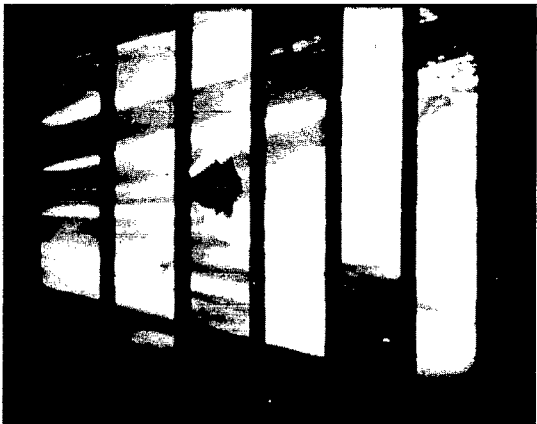
Figure 7.- Schlieren photographs of decelerator models at various x/d locations behind the X-15 model. $M = 4.65$.



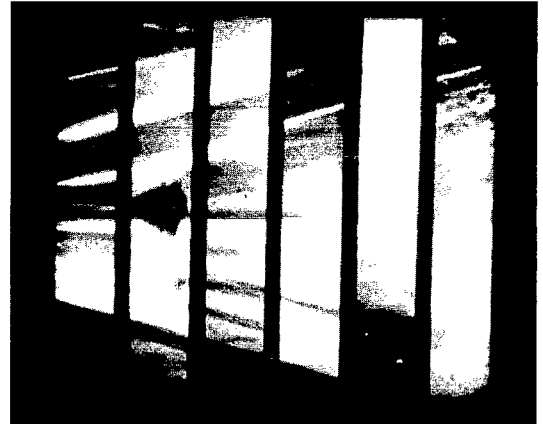
$x/d = 7.75$



$x/d = 5.18$



$x/d = 4.25$

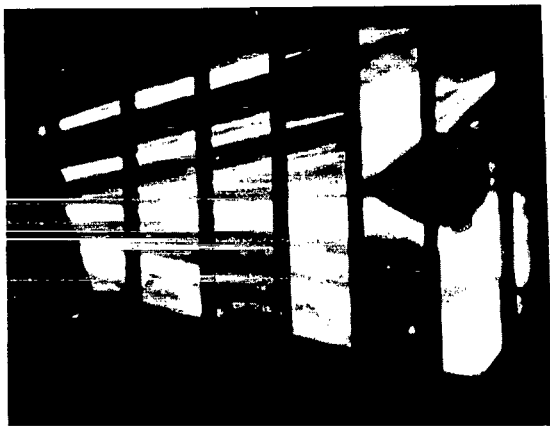


$x/d = 2.63$

(b) B2 self-inflatable configuration.

L-65-9026

Figure 7.- Continued.



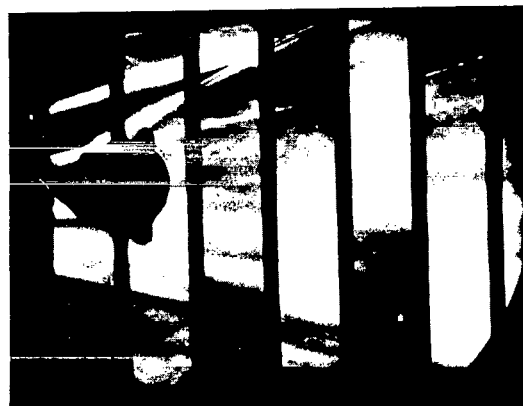
$x/d = 7.70$



$x/d = 4.28$



$x/d = 2.63$

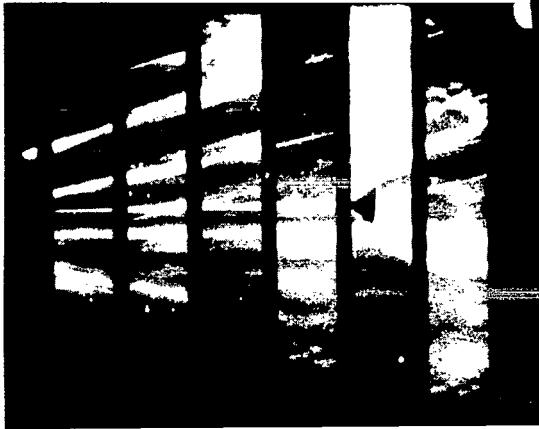


$x/d = 1.00$

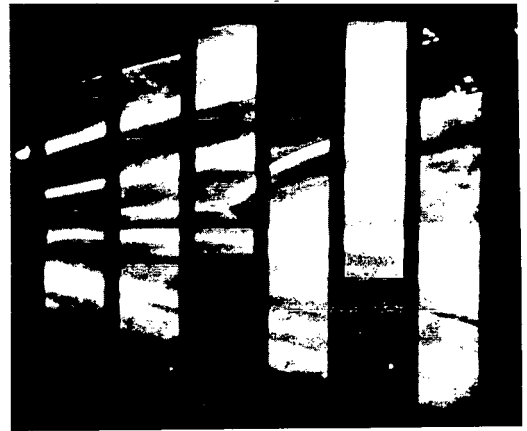
(c) B₃ self-inflatable configuration.

L-65-9027

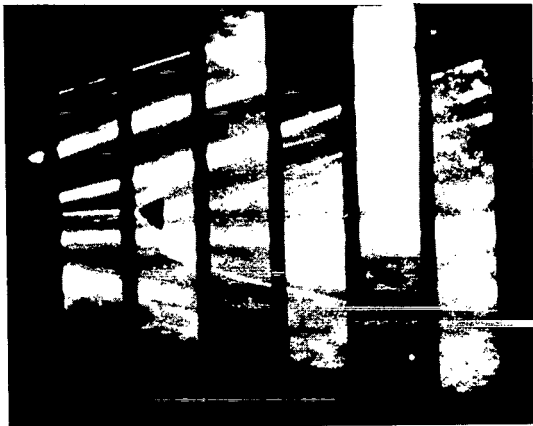
Figure 7.- Continued.



$x/d = 7.88$



$x/d = 5.30$



$x/d = 2.88$

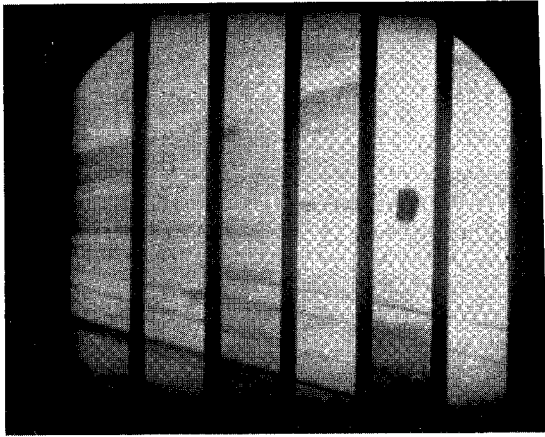


$x/d = 1.85$

(d) 80° rigid cone.

L-65-9028

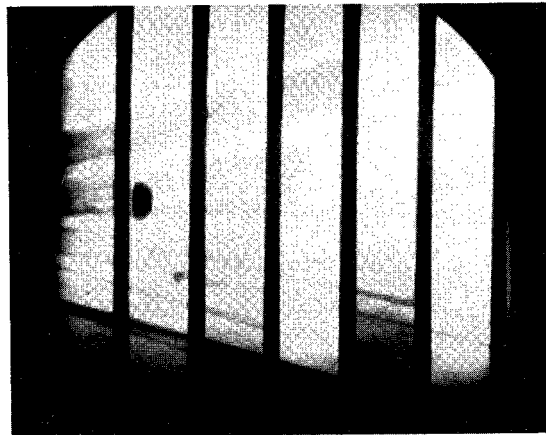
Figure 7.- Continued.



$x/d = 6.65$



$x/d = 2.85$

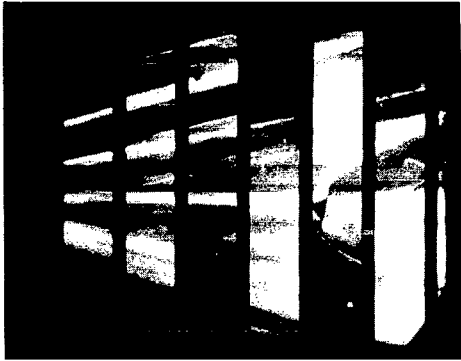


$x/d = 1.03$

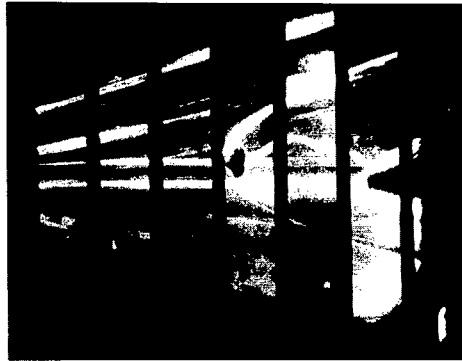
(e) Supersonic parachute.

L-65-9029

Figure 7.- Continued.



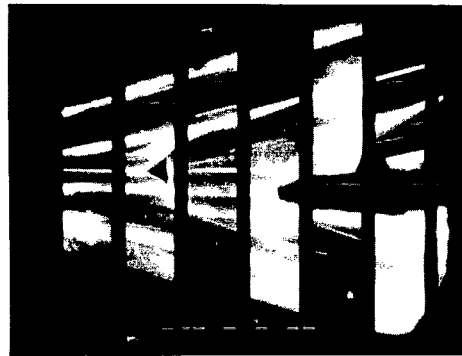
$x/d = 7.60$



$x/d = 6.33$



$x/d = 4.35$



$x/d = 3.35$



$x/d = 2.80$



$x/d = 1.53$

(f) Tension shell.

L-65-9030

Figure 7.- Concluded.

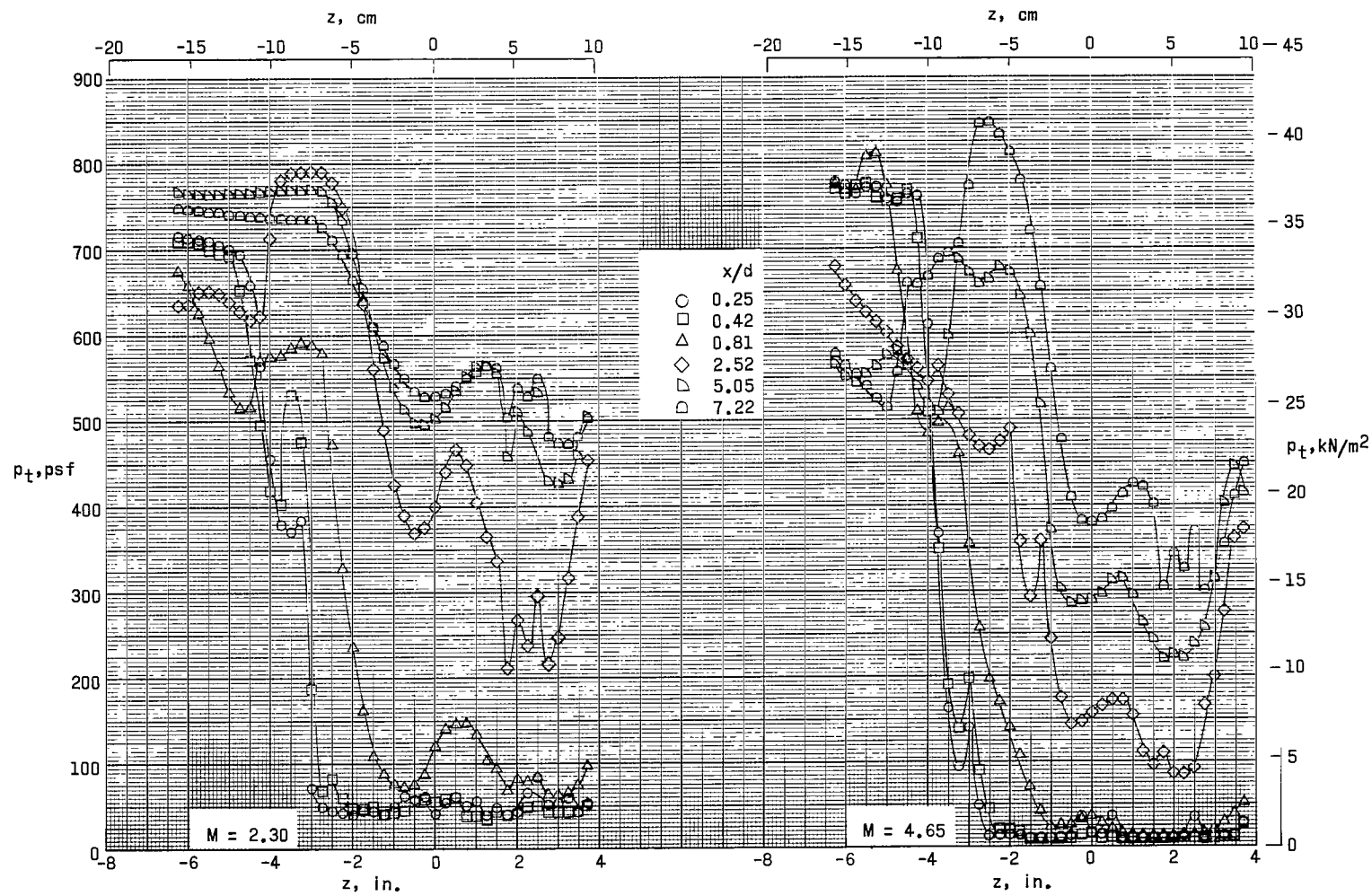
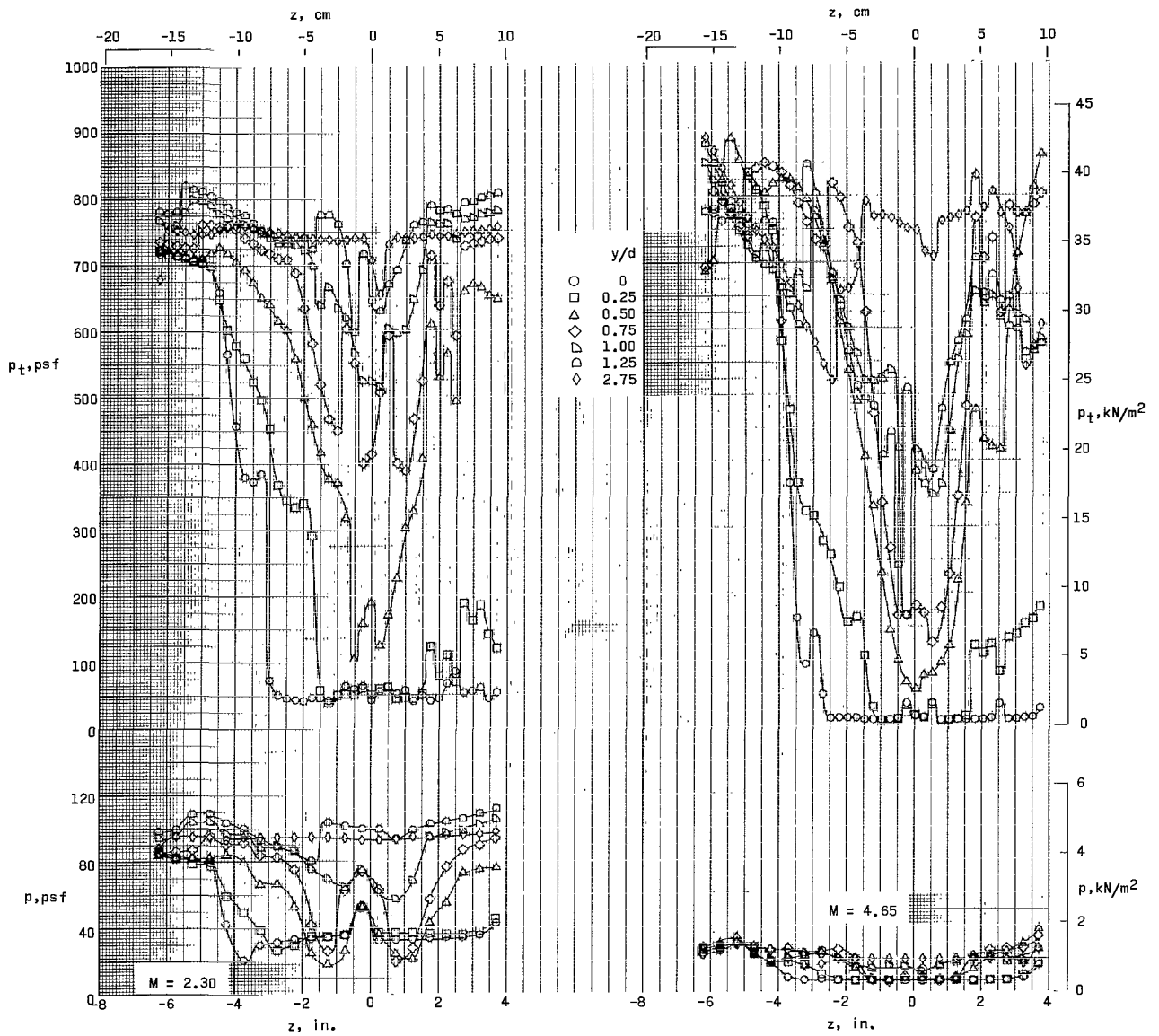
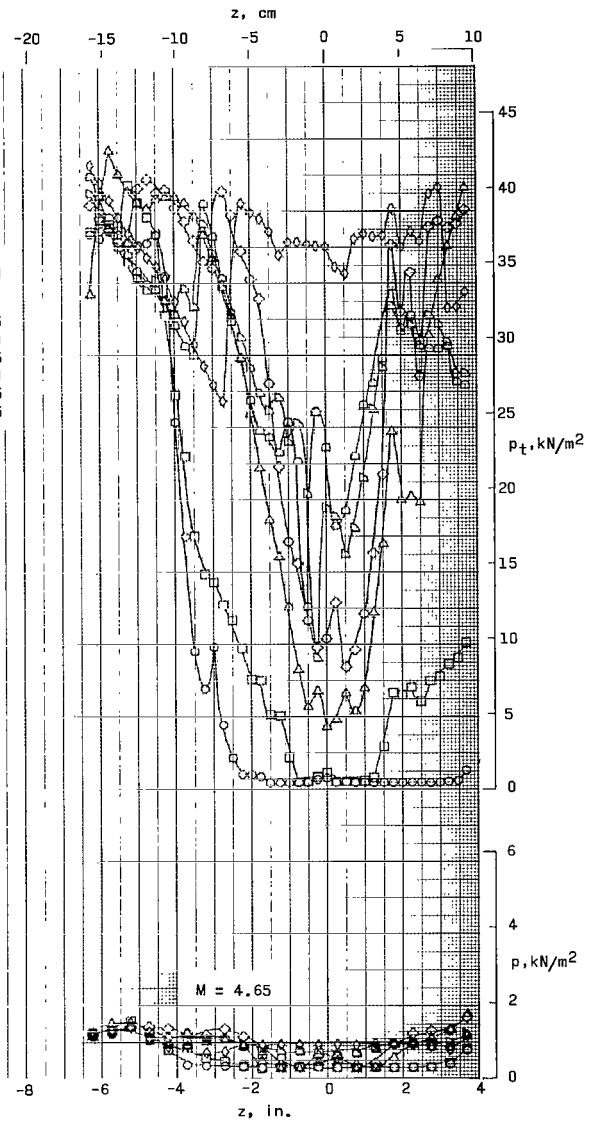
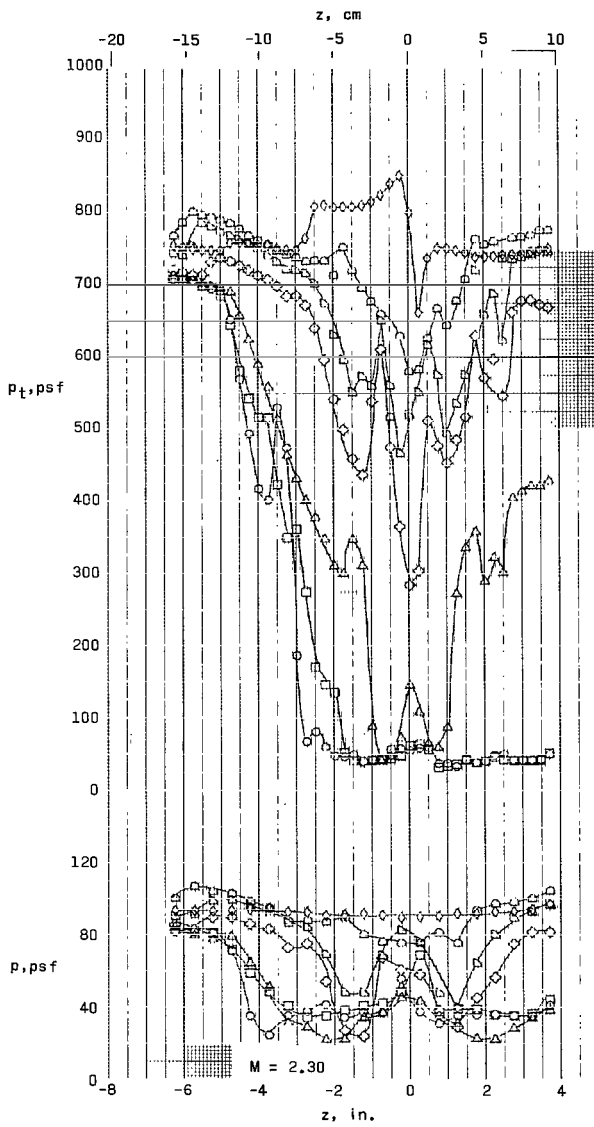


Figure 8.- Total-pressure distribution in vertical plane of symmetry at various x/d locations behind the X-15 model. $y/d = 0$.



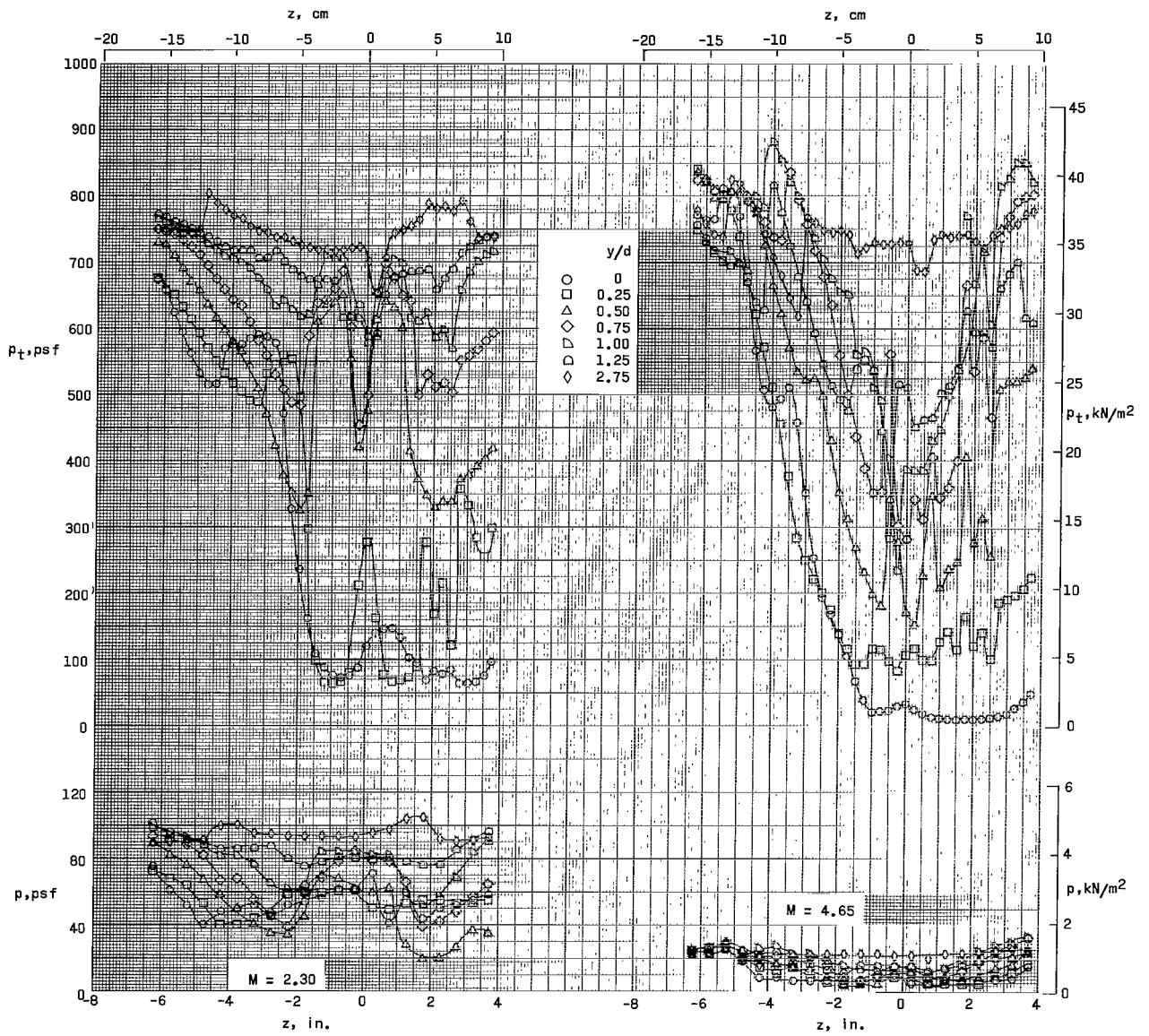
(a) $x/d = 0.25$.

Figure 9.- Vertical total- and static-pressure distribution at various y/d locations.



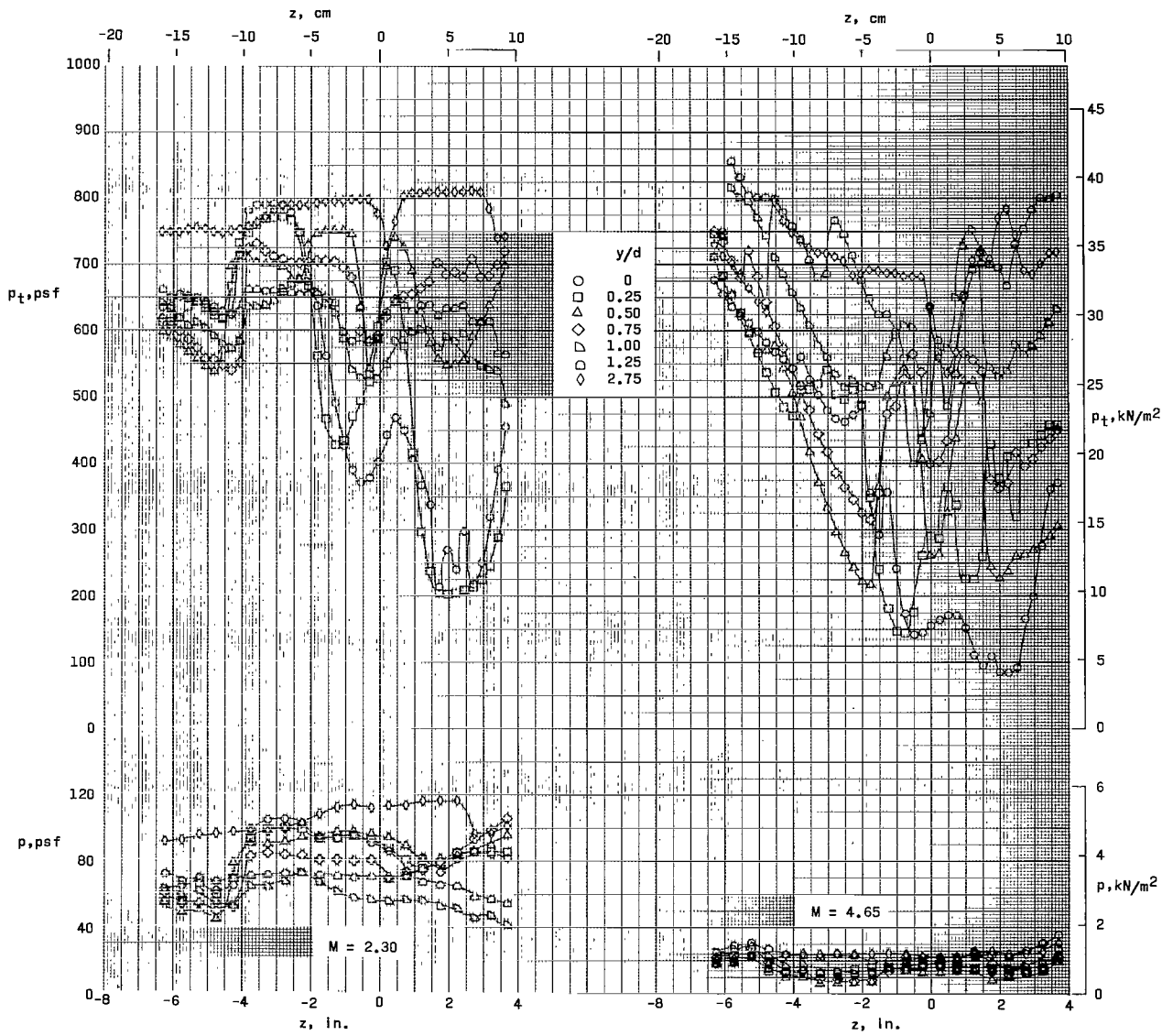
(b) $x/d = 0.42$.

Figure 9.- Continued.



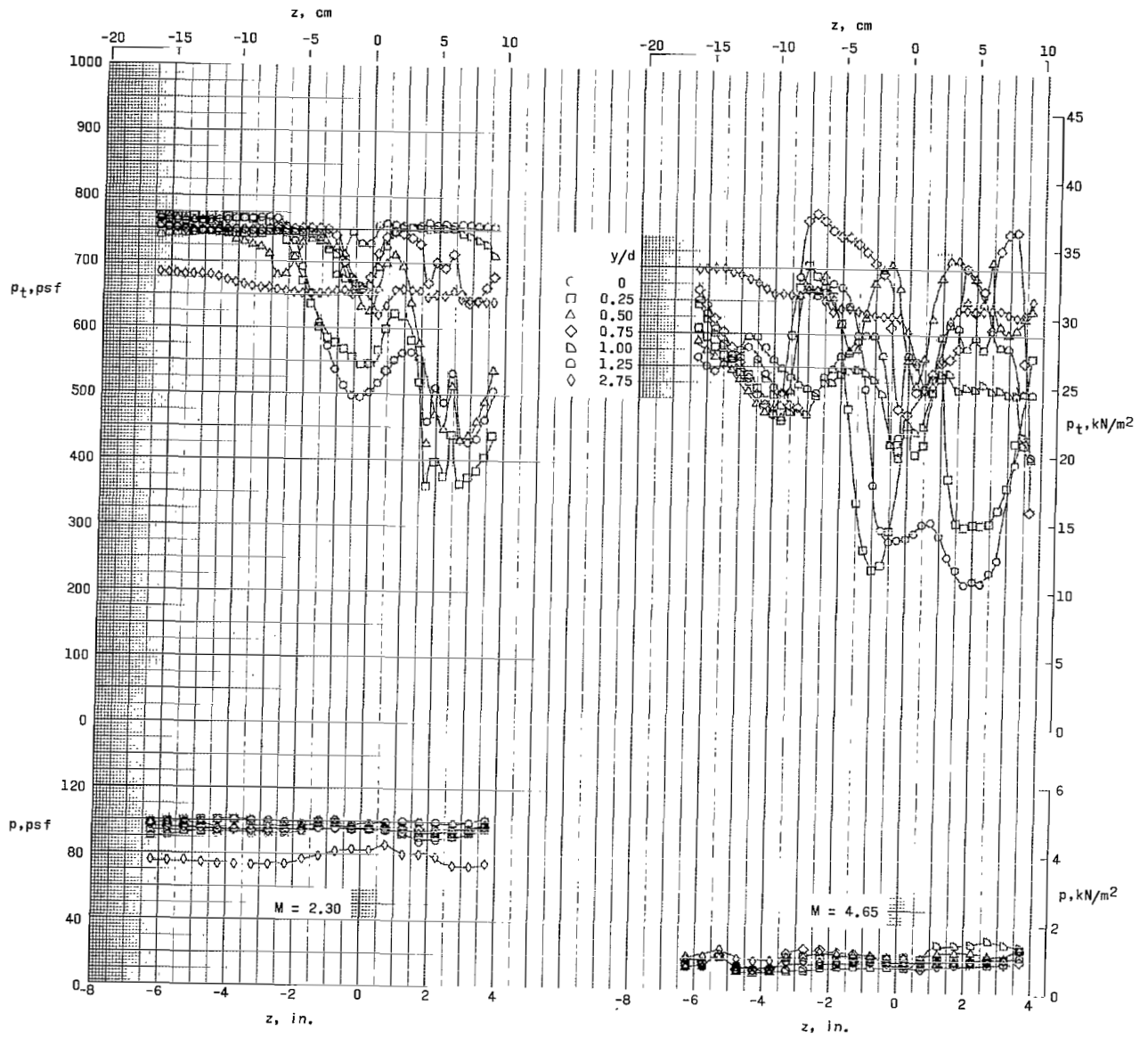
(c) $x/d = 0.81$.

Figure 9.- Continued.



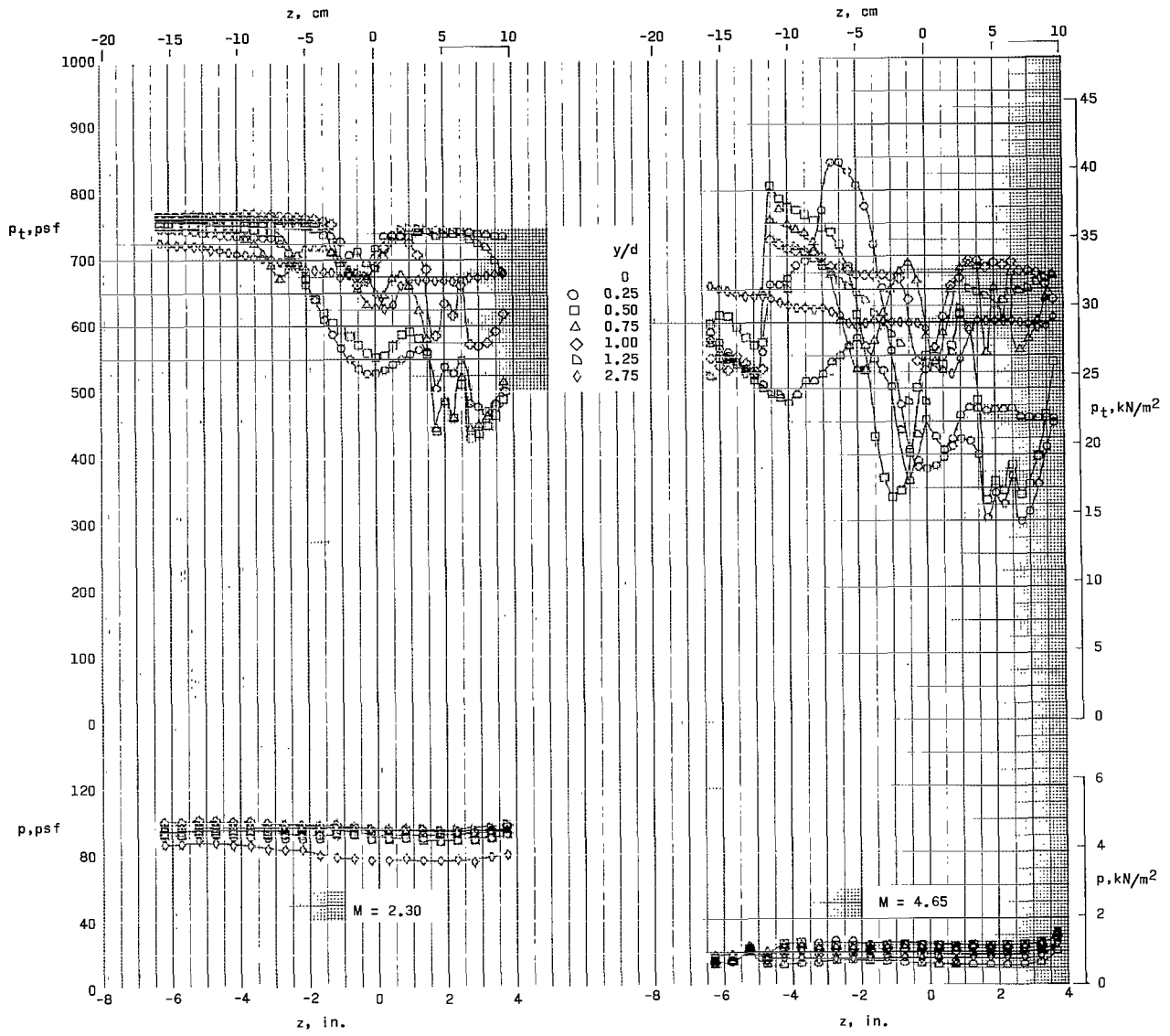
(d) $x/d = 2.52$.

Figure 9.- Continued.



(e) $x/d = 5.05$.

Figure 9.- Continued.



(f) $x/d = 7.22$.

Figure 9.- Concluded.

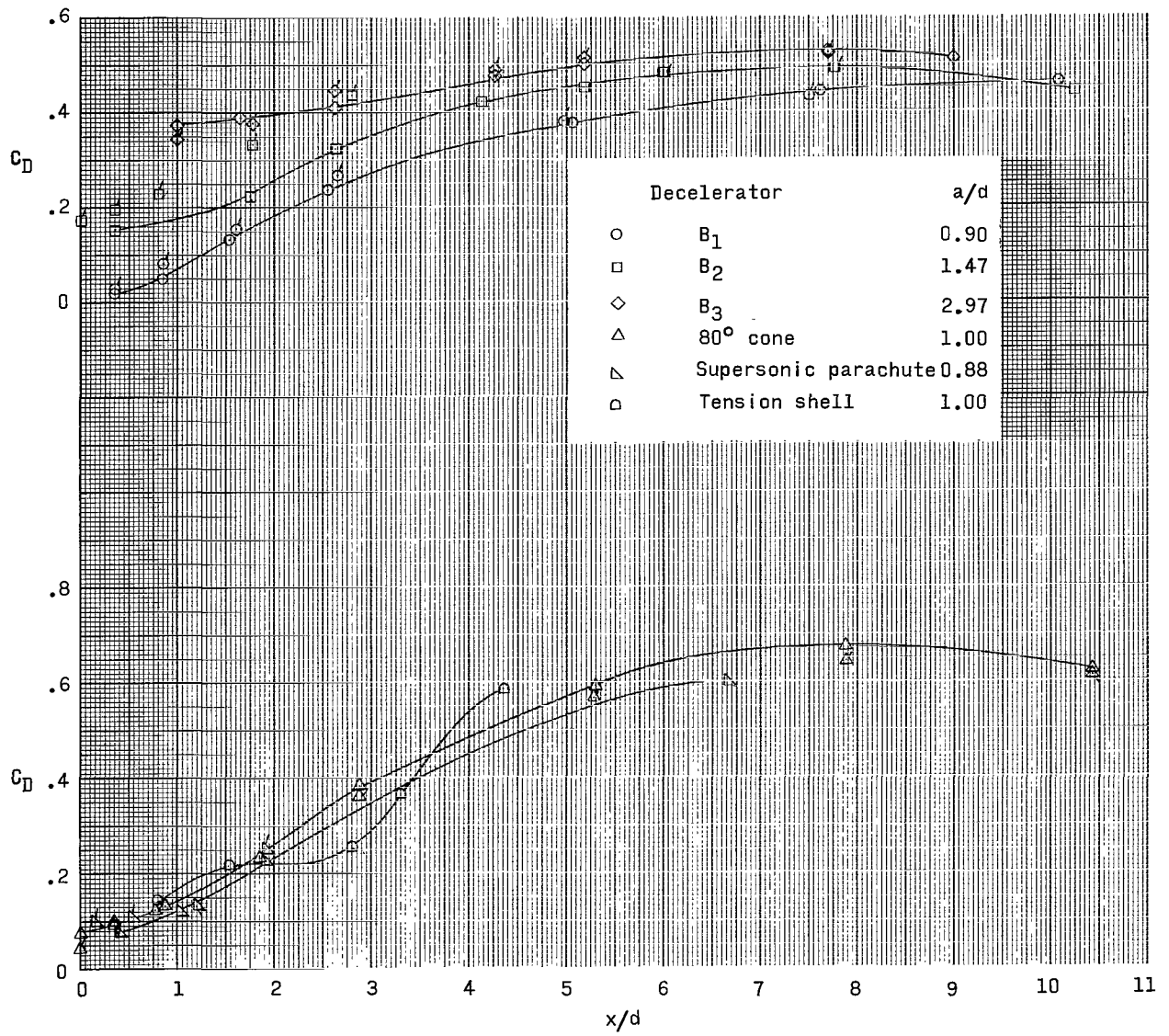


Figure 10.- Variation of drag coefficient with x/d for the decelerator configurations. $M = 4.65$. (Ticked symbols indicate data taken as x/d is decreased.)

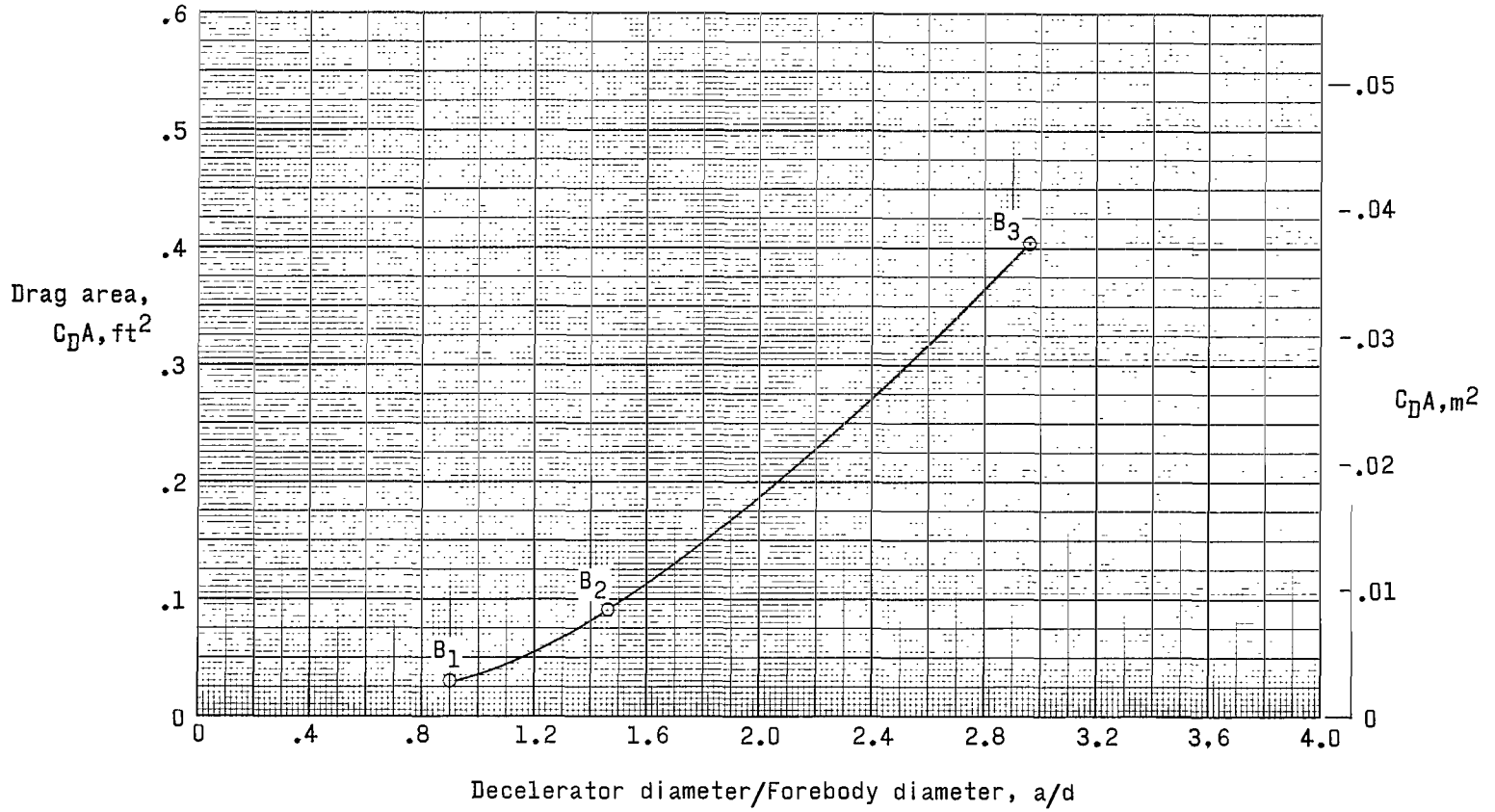


Figure 11.- Effects of ballute decelerator size on drag area. $x/d = 7.70$; $M = 4.65$.

"The aeronautical and space activities of the United States shall be conducted so as to contribute . . . to the expansion of human knowledge of phenomena in the atmosphere and space. The Administration shall provide for the widest practicable and appropriate dissemination of information concerning its activities and the results thereof."

—NATIONAL AERONAUTICS AND SPACE ACT OF 1958

NASA SCIENTIFIC AND TECHNICAL PUBLICATIONS

TECHNICAL REPORTS: Scientific and technical information considered important, complete, and a lasting contribution to existing knowledge.

TECHNICAL NOTES: Information less broad in scope but nevertheless of importance as a contribution to existing knowledge.

TECHNICAL MEMORANDUMS: Information receiving limited distribution because of preliminary data, security classification, or other reasons.

CONTRACTOR REPORTS: Technical information generated in connection with a NASA contract or grant and released under NASA auspices.

TECHNICAL TRANSLATIONS: Information published in a foreign language considered to merit NASA distribution in English.

TECHNICAL REPRINTS: Information derived from NASA activities and initially published in the form of journal articles.

SPECIAL PUBLICATIONS: Information derived from or of value to NASA activities but not necessarily reporting the results of individual NASA-programmed scientific efforts. Publications include conference proceedings, monographs, data compilations, handbooks, sourcebooks, and special bibliographies.

Details on the availability of these publications may be obtained from:

SCIENTIFIC AND TECHNICAL INFORMATION DIVISION
NATIONAL AERONAUTICS AND SPACE ADMINISTRATION

Washington, D.C. 20546